Chemical Science

ROYAL SOCIETY OF CHEMISTRY

EDGE ARTICLE

View Article Online
View Journal | View Issue

Cite this: *Chem. Sci.*, 2024, **15**, 3372

All publication charges for this article have been paid for by the Royal Society of Chemistry

Received 28th November 2023
Accepted 23rd January 2024

DOI: 10.1039/d3sc06365h

rsc.li/chemical-science

Tumor targeted alpha particle therapy with an actinium-225 labelled antibody for carbonic anhydrase IX†

Katherine A. Morgan,[a] Christian W. Wichmann,[bcd] Laura D. Osellame,[bc] Zhipeng Cao,[bc] Nancy Guo,[b] Andrew M. Scott[bcde] and Paul S. Donnelly*[a]

Selective antibody targeted delivery of α particle emitting actinium-225 to tumors has significant therapeutic potential. This work highlights the design and synthesis of a new bifunctional macrocyclic diazacrown ether chelator, H_2MacropaSqOEt, that can be conjugated to antibodies and forms stable complexes with actinium-225. The macrocyclic diazacrown ether chelator incorporates a linker comprised of a short polyethylene glycol fragment and a squaramide ester that allows selective reaction with lysine residues on antibodies to form stable vinylogous amide linkages. This new H_2MacropaSqOEt chelator was used to modify a monoclonal antibody, girentuximab (hG250), that binds to carbonic anhydrase IX, an enzyme that is overexpressed on the surface of cancers such as clear cell renal cell carcinoma. This new antibody conjugate (H_2MacropaSq-hG250) had an average chelator to antibody ratio of 4 : 1 and retained high affinity for carbonic anhydrase IX. H_2MacropaSq-hG250 was radiolabeled quantitatively with [^{225}Ac]Ac^{III} within one minute at room temperature with micromolar concentrations of antibody and the radioactive complex is stable in human serum for >7 days. Evaluation of [^{225}Ac]Ac(MacropaSq-hG250) in a mouse xenograft model, that overexpresses carbonic anhydrase IX, demonstrated a highly significant therapeutic response. It is likely that H_2MacropaSqOEt could be used to modify other antibodies providing a readily adaptable platform for other actinium-225 based therapeutics.

Introduction

Treatment of cancers is possible by systemic administration of either alpha (α^{2+}) or beta (β^-)-emitting radionuclides that selectively target active sites of disease and induce irreversible damage to DNA. The selectivity for cancer cells can be increased by attaching radionuclides to molecules or antibodies that bind to receptors that are over-expressed in tumor tissue compared to normal tissue. The use of radionuclides that emit β^- particles have been the most studied with respect to radionuclide therapy. The potential for radionuclide therapy is highlighted by the recent clinical approval of two radiopharmaceuticals based on β^- emitting lutetium-177, [^{177}Lu]Lu(DOTATATE) and [^{177}Lu]Lu(PSMA-617), for the treatment of somatostatin receptor-positive neuroendocrine tumors and metastatic castrate-resistant prostate cancer, respectively.[1–11]

Exposure of DNA and proteins to ionizing radiation causes lesions to the DNA that initiate downstream cellular signaling and, ultimately, cell death. Ionizing radiation also leads to the formation of free radicals, such as the hydroxyl radical that can hydroxylate biomolecules.[12] The formation of reactive free radical species is enhanced in the presence of oxygen. For hypoxic tumors, which are characterized by insufficient oxygen supply relative to the tumor, the low levels of oxygen reduce the efficacy of therapy with β-emitting radionuclides.[13]

Radionuclides that emit particles are potentially more effective in hypoxic environments as their cytotoxicity to solid tumors is independent of oxygen levels. As few as two α particles must traverse a cell nucleus to induce lethal lesions.[14,15] Radioactive decay by α-emission involves the emission of helium nuclei (two protons and two neutrons) from the nucleus. The range of the particles emitted by radionuclides in tissue depends on their Linear Energy Transfer (LET), a measure of the amount of energy transferred per unit length along the track of an ionizing particle (keV μm^{-1}) and the kinetic energy of the particle. The high LET α particles exhibit an extraordinary degree of efficacy. The α emitting actinium-225 radionuclide has the potential to assist in the treatment of unresponsive refractory tumors and hypoxic tumors.[13] Actinium-225 has

[a]*School of Chemistry and Bio21 Molecular Science and Biotechnology Institute, University of Melbourne, Melbourne, Australia*

[b]*Tumour Targeting Laboratory, Olivia Newton-John Cancer Research Institute, Melbourne, Australia*

[c]*School of Cancer Medicine, La Trobe University, Melbourne, Australia*

[d]*Department of Molecular Imaging and Therapy, Austin Health, Melbourne, Australia*

[e]*Department of Medicine, University of Melbourne, Melbourne, Australia. E-mail: pauld@unimelb.edu.au*

† Electronic supplementary information (ESI) available. See DOI: https://doi.org/10.1039/d3sc06365h

a radioactive half-life of 9.9 days and decays to bismuth-209 ($t_{1/2}$ = 1.9 × 10^{19} years) *via* the release of a total of four α particles ($E\alpha^{2+}$ = 5.9–8.4 MeV) and two β^- particles.[11,16]

Tumor hypoxia and general cellular oxygen homeostasis are maintained by the transcription factor hypoxia inducible factor 1 (HIF-1), which controls the expression of hundreds of genes.[17] The regulation of HIF involves O_2-dependent degradation of HIF-1a triggered by binding to the von Hippel–Lindau tumor suppressor protein (VHL).[18–22] Mutation and subsequent inactivation of the VHL gene is indicated in the pathogenesis of both hereditary and sporadic clear cell Renal Cell Carcinoma (ccRCC) leading to a hypoxic phenotype.[23] A downstream consequence of hypoxia is increased expression of Carbonic Anhydrase IX (CAIX), a zinc metalloenzyme that plays an integral role in the adaption of the tumor microenvironment to low-oxygen. Greater than 75% of primary and metastatic RCC express the CAIX protein,[24] and CAIX is over-expressed in 94% of ccRCC tumors due to the mutational loss of VHL protein.[25–27] Several other tumors, including glioblastoma, triple-negative breast cancer, ovarian cancer, and colorectal cancer, also overexpress CAIX on the tumor surface with relatively low levels or no expression in other tissues.[28,29] The high expression of CAIX on tumors compared to relatively low levels of expression in other tissue means the enzyme is a viable target for radionuclide therapy.

The monoclonal antibody, chimeric girentuximab (cG250), is selective for CAIX over different isoforms of carbonic anhydrase and the antibody binds to the extracellular proteoglycan-like domain.[25,30] Clinical studies with cG250 radiolabeled with lutetium-177, [^{177}Lu]Lu(DOTA-cG250), (DOTA = 1,4,7,10-tetraazacyclododecane-*N*,*N*′,*N*″,*N*‴-tetraacetic acid) demonstrated a promising response in patients with progressive metastatic ccRCC.[31] High expression of CAIX is often associated with a hypoxic tumor microenvironment reducing the formation of reactive oxygen species upon exposure to a β-emitting radionuclide such as [^{177}Lu]Lu^{III}.

In this work, we aim to use a newly available humanized variant of girentuximab (hG250) to selectively deliver α-emitting [^{225}Ac]Ac^{III} to tumors that over-express CAIX and are typically hypoxic, and therefore more radioresistant. The energy of α particles is sufficient to directly damage DNA in low oxygen concentrations.[32] The potential of using actinium-225 for radioimmunotherapy was realized in seminal preclinical work.[33–36] This initial work, as well as recent work with hG250,[37] used DOTA as a chelator for actinium-225. The thermodynamic stability of metal ion complexes of DOTA is inversely related to the ionic radius of the metal ion, meaning that larger cations such as Ac^{III} are likely to form less stable complexes with DOTA.[38] Complexation of [^{225}Ac]Ac^{III} with DOTA requires heating above 50 °C which often denatures antibodies or the use of high concentrations of antibody conjugate. While it is possible to radiolabel DOTA-antibody conjugates with [^{225}Ac]Ac^{III}, the prolonged radiolabeling times required and the low radiochemical yields are sub-optimal.

The 4,13-diaza-18-crown-6 ether with two picolinate pendant arms, *N*,*N*′-bis[(6-carboxy-2-pyridil)methyl]-4,13-diaza-18-crown-6 was shown to be highly selective for the larger, early lanthanides.[40] Pioneering work by Radchenko and Wilson identified the diazacrown ether, called H_2Macropa (Fig. 1a), as a superior ligand for coordination to [^{225}Ac]Ac^{III}.[39] The H_2Macropa ligand and its derivatives can be labeled with [^{225}Ac]Ac^{III} at room temperature in 5 minutes using sub-micromolar ligand concentrations. Addition of an isothiocyanate functional group to one of the picolinate arms to give H_2Macropa-NCS (Fig. 1b) provides a point of functionalization to attach peptides or proteins to the macrocyclic framework.[39] H_2Macropa is a better ligand than DOTA for [^{225}Ac]Ac^{III} but the *para*-isothiocyanate substituted pyridine in H_2Macropa-NCS is susceptible to hydrolysis, as the electron-withdrawing *ortho*-carboxylic acid functional group significantly increases the reactivity of the isothiocyanate functional group, reducing the shelf life of the compound.[41,42] The reaction of metal-binding ligands bearing isothiocyanate functional groups with the amine groups of lysine residues in antibodies leads to thiourea linkages that are relatively hydrophobic, and this can lead to aggregation of the antibody and loss of function.

Here, we report the development of a one-pot synthesis of non-symmetric substituted variants of H_2Macropa and the incorporation of a squaramide ethyl ester functional group separated from the macrocycle by a short oligo(ethylene glycol) linker, H_2MacropaSqOEt (Fig. 1c). In contrast to isothiocyanates, squaramide ethyl esters are stable with respect to hydrolysis and have a long shelf life.[44] Squaramide ethyl esters react selectively with amines of lysine residues present in antibodies at room temperature and in aqueous solutions (Scheme 1). The resulting diamide is very stable due to the aromaticity of the resulting vinylogous amides.

Squaramide functional groups are also considered isosteres for a variety of carboxylate groups, including carboxylic acids and amino acids.[45] This leads to bioconjugates of increased stability compared to thioureas formed from the isothiocyanate coupling. The new H_2MacropaSqOEt was then used to conjugate the macrocycle to hG250. The new immunoconjugate was radiolabeled to give [^{225}Ac]Ac(MacropaSq-hG250) and the

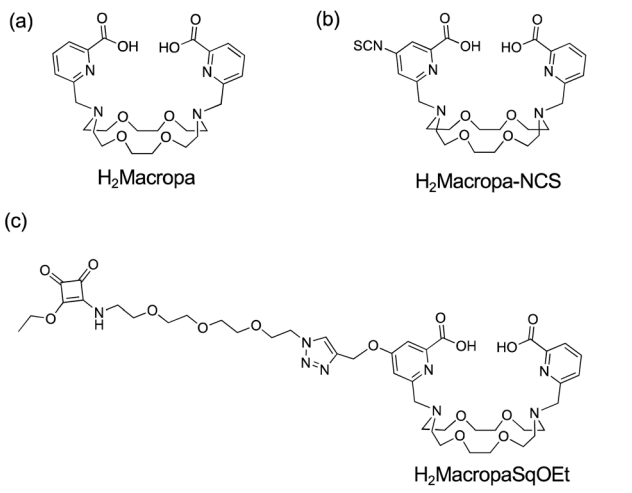

Fig. 1 Structure of (a) H_2Macropa, (b) H_2Macropa-NCS from Radchenko and Wilson,[39] and (c) H_2MacropaSqOEt (this work).

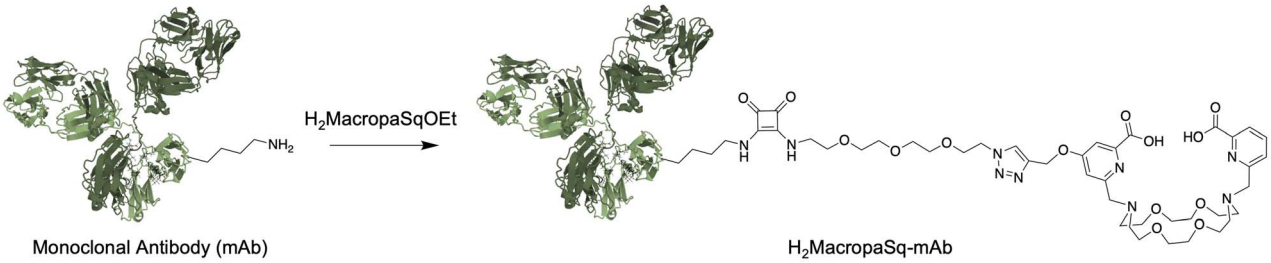

Scheme 1 Schematic representation of the conjugation chemistry of squaramides. The squaramide ethyl ester functional group in H_2-MacropaSqOEt permits bioconjugation to antibodies through selective reactions with the lysine residues of antibodies and forms a stable vinylogous squaramide linkage.

therapeutic efficacy of the radioimmunoconjugate was evaluated in a SK-RC-52 animal model of ccRCC.

Results

It is preferable to have a non-symmetric macrocycle with only one point for conjugation for the conjugation of macrocycles to antibodies. A challenge in producing non-symmetrical 4,13-diaza-18-crown-6 ether ligands is the formation of disubstituted as well as monosubstituted products even when the *N*-alkylation reactions are conducted at high dilution (Scheme 2a). In this work, we followed a similar procedure to Radchenko and Wilson following the literature synthesis of methyl-6-chloromethylpyridine-2-carboxylate,[43] but replaced the amine/isothiocyanate functional group on one picolinic acid functional group with an alkyne-bearing prop-2-yn-1-yloxy functional group in the 4-position of the picolinate functional group to give compound **3**. This alkyne group was installed for further modification using copper(I)-catalyzed azide–alkyne cycloaddition (CuAAC) reactions.

The synthesis of **3** proceeded in four steps. The carboxylic acid functional groups of chelidamic acid were esterified. Ethyl esters were chosen based on the solubility of chelidamic acid in ethanol (76%). To incorporate an alkyne functional group into the metal chelator, propargyl bromide was reacted with the hydroxyl group at the 4-position of the chelidamic acid (68%). After incorporating the alkyne functional group, a reduction with sodium borohydride and chlorination of the resulting primary alcohol with thionyl chloride yielded **3** (58% yield over two steps) which would be reacted with diaza-18-crown-6. During the progress of this work, an independent synthesis of compound **5** was published.[46]

We investigated two different synthetic routes to form non-symmetrically substituted diaza-18-crown-6, route one and route two. In our first iteration of route one (Scheme 2, method A) the sequential *N*-alkylation of the diaza-18-crown-6 with compounds **2** and **3** required long reaction times (>40 hours per reaction). Following the first *N*-alkylation, the mono-substituted product (**4**) was purified by reverse-phase high-performance liquid chromatography (RP-HPLC). A second *N*-alkylation with compound **3** only resulted in low synthetic yields of the desired compound **5** (Scheme 2b, method A: 7–19%), despite the relatively long reaction time of ~40 hours due to the hydrolysis of the starting material **3**. The low yields using method A motivated us to pursue an alternative approach using microwave irradiation (method B). The microwave-assisted secondary *N*-alkylation of **4** in the presence of *N*,*N*-diisopropylethylamine (DIPEA) proceeded with superior yields (Scheme 2b, method B). The accelerated reaction time by microwave irradiation achieved significantly higher yields without any detectable breakdown of the starting material. Purification of this reaction mixture by semi-preparative HPLC allowed recovery of precious starting material and compound **5** in 52% yield.

The synthesis of compound **5** was further optimized in a one-pot synthesis (Scheme 2c, route two). Microwave irradiation of all three starting materials for 1 hour at 85 °C, followed by purification by RP-HPLC, isolated the compound **5** in 48% yield. Semi-preparative HPLC of the crude reaction mixture allowed for the straightforward separation of the desired macrocycle **5**, as well as a variant that contains two alkyne functional groups (**5_2**), (Fig. S1†) and recovery of any unreacted starting materials. The variant with two alkyne functional groups (**5_2**) is of use in preparing bivalent ligands where two targeting agents are coupled to a single chelator (Fig. S2†) The one-pot, microwave irradiation route benefits from significantly shorter reaction times (1 *vs.* ~80 hours), one less separation step by RP-HPLC reduces both the overall time involved and mobile phase consumption (acetonitrile/trifluoroacetic acid) and results in relatively high isolated yields. The methyl and ethyl esters of compound **5** were hydrolyzed quantitively with NaOH in a mixture of dichloromethane and methanol. The crude solution was neutralized and then purified by semi-preparative HPLC, which allowed for the isolation of the diacid, compound **6** in > 85% yield (Scheme 2, route one and two).

The terminal alkyne on the metal chelator (**6**) was reacted with the aliphatic azide on the short oligo(ethylene glycol) chain with a pendant squaramide ethyl ester (**7**) and proceeded using a copper(I)-catalyzed azide–alkyne cycloaddition (Scheme 2d).[47,48] Copper(II) sulfate pentahydrate was reduced with sodium ascorbate *in situ* to the active copper(I) species in the presence of tris((1-benzyl-4-triazolyl)methyl)amine (TBTA) as an additive to facilitate the quantitative, regioselective formation of the 1,2,3-triazole. The remaining copper(I/II) was removed with excess Na_2EDTA, and the crude reaction mixture was purified *via* semi-preparative HPLC to give compound **8** H_2-MacropaSqOEt, in 41% yield. The compound was characterized

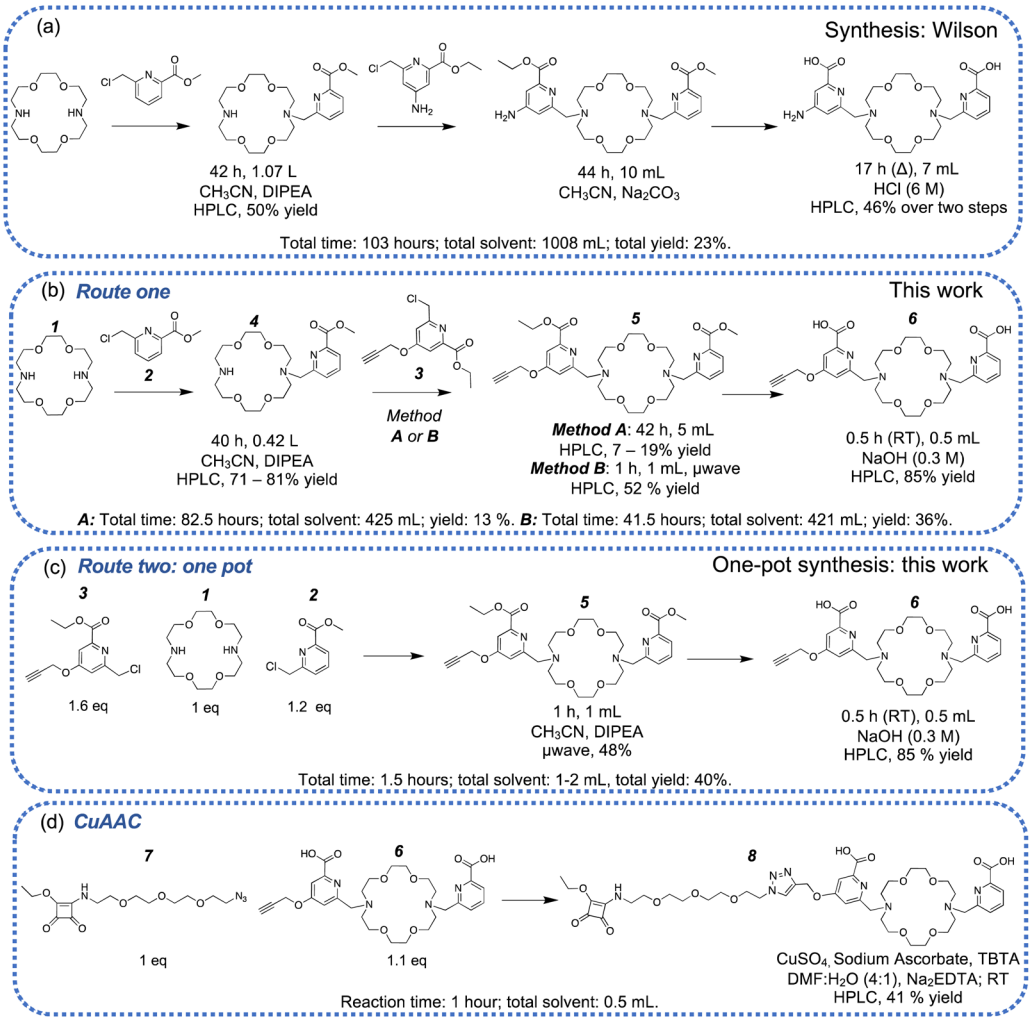

Scheme 2 Different reaction conditions: including reaction time, solvent volume, and reported yields. (a) Published synthesis and reaction conditions reported by Wilson,[39] (b) the original synthetic strategy used in this work with sequential *N*-alkylation, method A used reflux, method B used microwave irradiation (μwave), (c) an improved one-pot microwave-assisted synthesis, (d) the synthesis of H_2MacropaSqOEt.

by RP-HPLC and high resolution ESI-MS where the major peak is attributed to the doubly protonated $[M + 2H]^{2+}$ adduct with an $m/z = 465.2161$. The ^{1}H NMR spectrum of H_2MacropaSqOEt is as expected with six downfield resonances corresponding to the five aromatic hydrogen atoms as part of the two pyridyl rings and one hydrogen at the 5-position of the 1,2,3-triazole (δ 8.24 ppm, Fig. S3†). The presence of isomers due to the vinylogous ethyl ester is evident in the resonances attributed to the –CH_2–CH_3 at δ 4.61 ppm, which integrates for two hydrogens and appears as a multiplet as a consequence of the two overlapping quartets. The corresponding –CH_3 environment integrates for three hydrogens but exists as a multiplet of two overlapping triplet signals at δ 1.52–1.55 ppm. The ligand, H_2MacropaSqOEt is stable when stored at 4 °C for >18 months as confirmed by analysis by ESI-MS and RP-HPLC (Fig. S4–S5†).

Conjugation of H_2MacropaSqOEt to girentuximab

The deconvoluted intact protein electrospray mass spectrum (ESI-MS) of the hG250 antibody has a signal at $m/z = 147\,568$ Daltons with different degrees of glycosylation resulting in peaks with a sequential increase in m/z of 160 Daltons (Da) (Fig. 2a). The reaction of H_2MacropaSqOEt (~15 equivalents) with hG250 in borate buffer (pH 9.0) for 4 hours led to the conjugation of the macrocyclic chelator to the antibody. An average chelator : antibody ratio of 4 : 1 was estimated by ESI-MS with each addition of H_2Macropa-Sq resulting in an increase of 882 Da (Fig. 2a). Unreacted H_2MacropaSqOEt was removed by spin filtration with a size exclusion filter, and the antibody conjugate was recovered in sodium acetate buffer (0.15 M, pH 5.5) that is ideal for radiolabeling with $[^{225}Ac]Ac^{III}$. Analysis of the antibody conjugates by size exclusion chromatography showed no significant changes in the SE-HPLC of H_2-MacropaSq-hG250 compared to the unmodified antibody (Fig. S6†). When the antibody conjugate, H_2MacropaSq-hG250 was stored at −20 °C, there was no change in the intact protein mass spectrum and SE-HPLC for at least 10 months. The binding of H_2MacropaSq-hG250 to CAIX was analyzed by an Enzyme-Linked Immunosorbent Assay (ELISA, Fig. 2b) and the

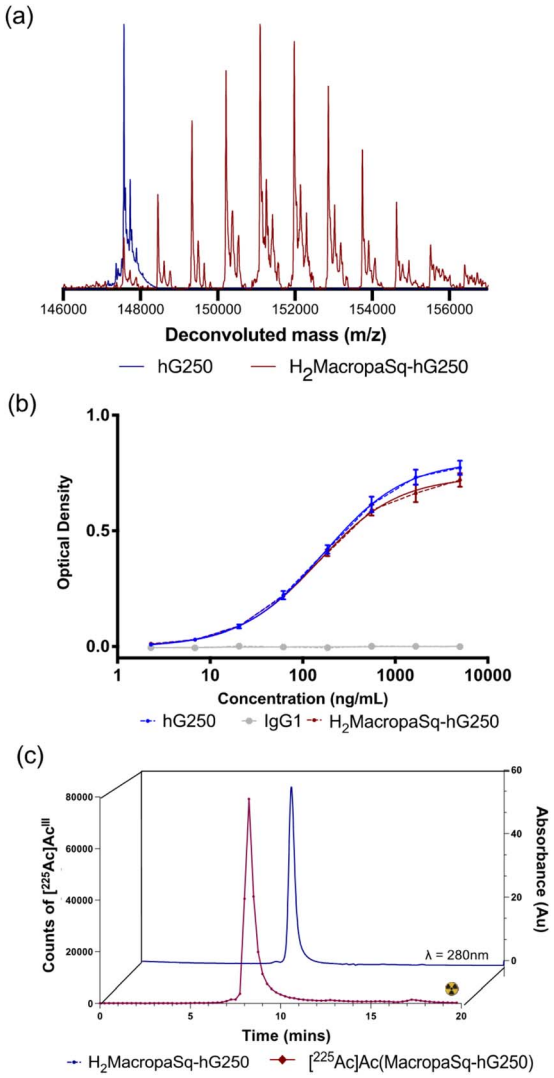

Fig. 2 (a) ESI-TOF deconvoluted mass spectra of unmodified girentuximab (hG250) overlaid with H_2MacropaSq-hG250 showing between 1–8 chelator attachments; (b) Elisa assay demonstrates that modifying the antibody with H_2MacropaSq functional groups does not impact the binding of hG250 to carbonic anhydrase IX (CAIX). The IgG1 control shows no binding to CAIX and is a suitable control antibody for further *in vitro* work. (c) SE-HPLC chromatogram of [^{225}Ac]Ac(MacropaSq-hG250). Radioactive fractions in red, compared to the UV trace of H_2MacropaSq-hG250 in blue ($\lambda = 280$ nm).

EC_{50} value for H_2MacropaSq-hG250 ($EC_{50} = 170 \pm 23$ nM) is similar to the unmodified antibody, hG250 (150 ±20 nM).

Synthesis of [^{225}Ac]Ac(MacropaSq-hG250)

[^{225}Ac]Ac$(NO_3)_3$ (Oak Ridge National Laboratory) as a 'nitrate film' was reconstituted in HCl (0.2 M) and then neutralized with sodium acetate buffer (sodium acetate, 0.15 M, pH 5.5). Neutralized [^{225}Ac]Ac^{III} (370 kBq) was reacted with H_2MacropaSq-hG250 (10 μg) with a final antibody concentration of 1.5 μM. The radiochemical purity (RCP) of [^{225}Ac]Ac(MacropaSq-hG250) was measured after reaction times of 1, 5, 15, and 30 minutes, at an antibody concentration of both 1.5×10^{-6} M and 1.5×10^{-7} M in sodium acetate buffer (pH 5.5). At an antibody concentration of 1.5×10^{-6} M, quantitative radiolabeling was achieved within 1 minute. At a concentration of 1.5×10^{-7} M, quantitative radiolabeling was achieved within 5 minutes. An IgG isotype control, [^{225}Ac]Ac(MacropaSq-IgG1), was also prepared (Fig. S7†). Both [^{225}Ac]Ac(MacropaSq-hG250) and [^{225}Ac]Ac(MacropaSq-IgG1) were characterized by comparing their respective size exclusion-HPLC traces with the unlabeled antibody conjugates ($\lambda = 280$ nm) (Fig. 2c).

In vitro stability of [^{225}Ac]Ac(MacropaSq-hG250)

The immunoreactivity of [^{225}Ac]Ac(MacropaSq-hG250) was measured over seven days (day 0, 2, 7) in human serum (37 °C, Sigma Aldrich) and expressed as a percentage of the immunoreactivity towards SK-RC-52 cells. Non-specific binding was measured using an excess of unlabelled antibodies. The immunoreactivity of [^{225}Ac]Ac(MacropaSq-hG250) decreased from 99.9% to 86.9% over 7 days. Analysis by radioTLC of a sample of [^{225}Ac]Ac(MacropaSq-hG250) incubated in human serum at 37 °C revealed that the radiolabeled complex remains 97.8% intact even after 7 days (Fig. S8†). The stability of [^{225}Ac]Ac(MacropaSq-hG250) in the presence of a competing trivalent metal, La^{III}, and a high-affinity metal chelator, ethylenediaminetetraacetic acid (H_4EDTA) was determined. An excess of the trivalent metal La^{III} can transchelate actinium, which would cause the decomplexation of [^{225}Ac]Ac^{III}. The RCP (measured *via* radioTLC) of the [^{225}Ac]Ac(MacropaSq-hG250) at multiple time points (1 hour, day 1, day 2, and day 7) in the presence of varying excess (5×, 50×, 500×) of La^{III} and H_4EDTA was measured. The data indicate that in the vehicle only (PBS), the radiochemical purity is not affected, with >99% RCP at all time points. The addition of La^{III} and EDTA appears to only have minor effects on the RCP, and the RCP remains above 99% for La^{III} and above 98% for the competition experiments with EDTA (Table S1†).

Biodistribution [^{225}Ac]Ac(MacropaSq-hG250) in SK-RC-52 tumor xenografts

The biodistribution of [^{225}Ac]Ac(MacropaSq-hG250) in BALB/c mice bearing SK-RC-52 renal cell carcinoma tumor xenografts was measured over seven days (Fig. 3a) and is presented in terms of the percentage of injected activity per gram of tissue (% IA g^{-1}). Mice were injected with 14.8 kBq of [^{225}Ac]Ac(MacropaSq-hG250) supplemented with 30 μg of hG250 or 14.8 kBq [^{225}Ac]Ac(MacropaSq-IgG1) (with 30 μg of IgG1). As expected, post injection there is initial high uptake in the blood pool and normal organs.

Three days after injection there is a high degree of tumor uptake (21.2 ± 6.5% IA g^{-1}; 3 d post injection) and importantly with respect to potential therapeutic effects the radioactivity in the tumor is retained out to seven days after injection (21.4 ± 10.1% IA g^{-1}; 7 d post injection). The specificity of the tumor uptake of [^{225}Ac]Ac(MacropaSq-hG250) in SK-RC-52 tumor xenografts was confirmed by comparison with the isotype control antibody, [^{225}Ac]Ac(MacropaSq-IgG1), in the same

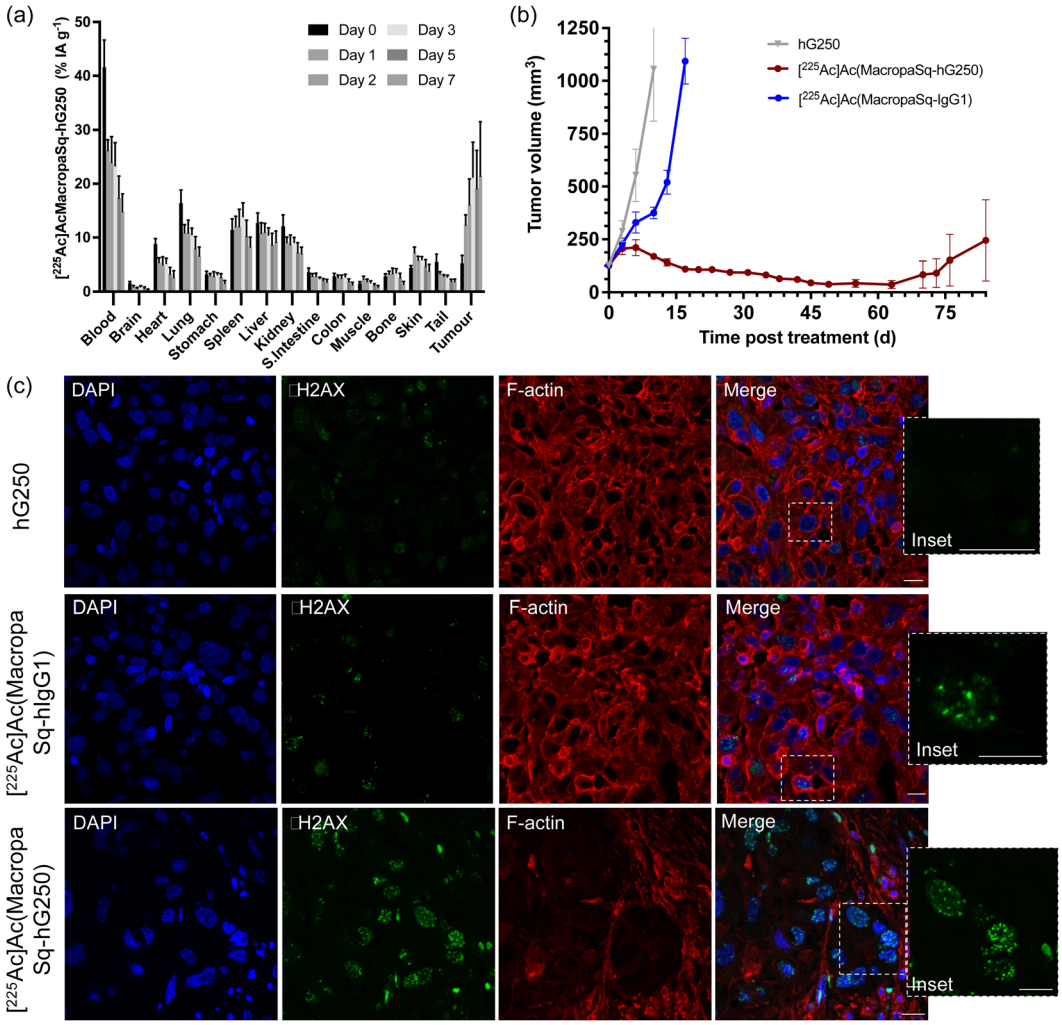

Fig. 3 (a) Biodistribution in BALB/c nude mice bearing SK-RC-52 tumors ($n = 5$). Mice were injected with 14.8 kBq of [^{225}Ac]Ac(MacropaSq-hG250) and sacrificed at days 0, 1, 2, 3, 5, 7; (b) mean tumor volume (mm^3) as a function of time post-treatment with [^{225}Ac]Ac(MacropaSq-hG250) (14.8 kBq, 30 μg), [^{225}Ac]Ac(MacropaSq-IgG1) (14.8 kBq, 30 μg) or hG250 (30 μg) in mice with SK-RC-52 tumor xenografts; (c) [^{225}Ac]Ac(MacropaSq-G250) induces double-strand DNA breaks in an SK-RC-52 tumor model. Confocal microscopy of SK-RC-52 tumors harvested on day 8 post-treatment were stained with DAPI (nuclei – blue) and immunostained with antibodies against γH2AX (ds DNA breaks – green) and F-actin (actin – red).

model where the tumor uptake 3 days post injection was only 3.6 ± 0.5% IA g^{-1} (Fig. S9†).

Therapeutic efficacy of [^{225}Ac]Ac(MacropaSq-hG250) in SK-RC-52 tumor xenografts

Administration of a single dose of [^{225}Ac]Ac(MacropaSq-hG250) (14.8 kBq, 30 μg hG250) significantly prolonged survival times when compared to administration of the radiolabelled control, [^{225}Ac]Ac(MacropaSq-IgG1) and non-radiolabelled hG250 control ($p \leq 0.0001$) (Fig. 3b). The therapeutic effect of the single administration of [^{225}Ac]Ac(MacropaSq-hG250) meant that 88% of the cohort were still alive until 84 days so a mean survival time could not be calculated (Fig. S10†). Eight days after administering either [^{225}Ac]Ac(MacropaSq-hG250), the isotype control [^{225}Ac]Ac(MacropaSq-IgG1), or non-radioactive hG250 the SK-RC-52 tumors were harvested and fixed with formalin. The tumor sections were treated with three different fluorophores to allow identification of the cell nucleus (λ_{em} 457 nm), F-actin microfilaments (λ_{em} 648 nm), and the presence of γH2AX phosphorylation, a marker of double-strand breaks (λ_{em} 568 nm) (Fig. 3c). Tumor sections following administration of [^{225}Ac]Ac(MacropaSq-hG250) had an average of 14.1 ± 1.6 H2AX phosphorylation foci per cell nucleus compared with 5.2 ± 0.8 foci per cell when administered the isotype control and 2.4 ± 0.5 foci per cell nucleus following administration of hG250 (Fig. S11†).

Representative spleen and kidney samples of the mice in each treatment group were collected seven days after administration as well as day 125 in the mice that were administered [^{225}Ac]Ac(MacropaSq-hG250) (Fig. S12–S13†). In the sections of the spleen collected on day 125, all structures are present (trabecula, white pulp, and red pulp) and are morphologically similar to the spleen samples acquired on day seven. The

kidneys have normal morphology in all treatment groups on day 7, and the day 125 kidneys for [^{225}Ac]Ac(MacropaSq-hG250) treated mice showed intact glomeruli but also some tubular atrophy (Fig. S13†).

Discussion

A new synthetic methodology for the preparation of non-symmetrically substituted diazacrown ether 'H_2Macropa' derivatives has been developed (Scheme 2, route 2). The advantages of this new methodology include a one-pot synthesis of compound **5** facilitated by microwave irradiation leading to relatively high isolated yields (48%). The optimization of the synthesis of these macrocycles may have positive implications for the development of this compound on large-scale synthesis. It is possible that this approach could be extended to other alkylation reactions, where microwave irradiation may facilitate higher yields and decreased reaction times.

The incorporation of the squaramide ethyl ester functional group to give H_2MacropaSqOEt permits bioconjugation to antibodies through selective reactions with the lysine residues of antibodies to form stable vinylogous squaramide linkages. Squaramide ethyl esters are stable with respect to hydrolysis and have a long shelf life and improved solubility in aqueous mixtures. The ligand H_2MacropaSqOEt is soluble in aqueous buffers, a significant advantage when aiming to modify monoclonal antibody conjugates. Optimal yields of the reaction of squaramide ethyl esters with antibodies were obtained after a reaction time of four hours. In our experience reactions with substituted isothiocyanates take less time (1–2 hours).

The reaction of hG250 with H_2MacropaSqOEt results in H_2-MacropaSq-hG250 with an average chelator to antibody ratio of 4 : 1 that retains affinity for CAIX as demonstrated by an ELISA assay (Fig. 2b) and there is no evidence of aggregation as measured by SE-HPLC (Fig. 2c). H_2MacropaSq-hG250 is stable when stored at −20 °C in radiolabeling buffer. The squaramide conjugate offers potential advantages over antibody conjugates prepared with the isothiocyanate derivative, H_2Macropa-NCS, as the presence of the electron-withdrawing picolinate substituent makes the –NCS functional group significantly more reactive and prone to hydrolysis.[41]

H_2MacropaSq-hG250 is radiolabeled quantitatively with [^{225}Ac]Ac^{III} within one minute at an antibody concentration of 1.5×10^{-6} M. When [^{225}Ac]Ac(MacropaSq-hG250) is stable in human serum for at least 7 days and when challenged with an excess of La^{III} and H_4EDTA. The high stability of [^{225}Ac]Ac(MacropaSq-hG250) demonstrated here is consistent with the results reported by Wilson and Radchenko on derivatives of [^{225}Ac]Ac(Macropa-NCS).[39]

Administration of [^{225}Ac]Ac(MacropaSq-hG250) (14.8 kBq) to SK-RC-52 tumor xenograft-bearing mice had a dramatic therapeutic effect consistent with high tumor uptake and retention. Two out of five mice (40%) experienced a complete response, with tumor volumes unable to be measured in the two mice after day 70 and the other three mice (60%) exhibited a significant partial response. An overall survival rate of 88% was demonstrated through the first 84 days of the study. Furthermore, 74% of the cohort remained alive even at 119 days after treatment.

The energy released in the decay of α-particles can induce double strand breaks in DNA that are harder to repair than single-strand breaks.[49–54] Exposure of DNA to ionizing radiation leads to phosphorylation of the H2AX histone serine-139 to form γH2AX which is a marker of double-strand breaks.[55,56] The phosphorylation is rapid and occurs within minutes of exposure to ionizing radiation and typically reaches a maximal level one hour after irradiation. These γH2AX foci are proportional to the number of DNA breaks.[57] Due to the signaling of downstream DNA repair factors, the number of foci generally decreases after 24 hours. After this time, the remaining foci presumably represent unrepairable double-strand breaks.[58–61] Tumor sections treated with 14.8 kBq of [^{225}Ac]Ac(MacropaSq-hG250) show significant DNA damage, evident by the presence of many γH2AX foci, including complex clustered DNA damage Fig. 3c.[59,62]

An ongoing challenge in the clinical implementation of α-particle therapy is to effectively balance therapeutic efficacy with off-target toxicity caused by exposure of healthy organs to the potent cytotoxic radionuclide. Weight loss in mouse models is a common and often dose-limiting side effect of anti-cancer therapies.[63] Administration of [^{225}Ac]Ac(MacropaSq-hG250) (14.8 kBq) initially led to a small decline in body weight but ten days post injection the mean body weight of the mice returned to their approximate initial weight. In comparison, administration of a similar amount of radioactivity of the DOTA conjugate, [^{225}Ac]Ac(DOTA-hG250) (15 kBq) in non-tumor bearing mice led to four out of six mice (66%) being culled due to significant weight loss (>18%).[37] A significant contribution to the off-target toxicities of α-particle therapy is radiation induced damage to the kidneys. Histologic analysis of kidney samples at day 125 of [^{225}Ac]Ac(MacropaSq-hG250) treated mice revealed some tubular atrophy but less pronounced than what was reported following administration of a similar dose of the DOTA variant, [^{225}Ac]Ac(DOTA-hG250).[37] Kidney toxicity following administration of [^{225}Ac]Ac^{III} is often attributed to accumulation of unchelated daughter radionuclide [^{213}Bi]Bi in the organ.[37] It is speculated that in this work the use of H_2-MacropaSq rather than DOTA as a chelator for [^{225}Ac]Ac^{III} led to a reduced accumulation of [^{213}Bi]Bi in the kidneys, but confirmation of this hypothesis requires further study.

Conclusions

A new high yielding one-pot microwave assisted synthetic approach for the preparation of non-symmetric functionalized diazacrown ether ligands has been developed. This new methodology was used to prepare a new bifunctional variant of H_2-Macropa with a pendant diethyl squarate ester, H_2MacropaSqOEt. The new bifunctional ligand H_2-MacropaSqOEt was used to chemically modify the monoclonal antibody hG250, that binds to CAIX. Tumors that over-express CAIX are typically hypoxic and more resistant to conventional radiation therapy, and therefore candidates for α-particle therapy. The antibody conjugate, H_2MacropaSq-hG250 can be

radiolabeled with [^{225}Ac]Ac^{III} at room temperature within 1 minute to give [^{225}Ac]Ac(MacropaSq-hG250) in excellent radiochemical yields. Treatment of mice with SK-RC-52 tumor xenografts with [^{225}Ac]Ac(MacropaSq-hG250) (14.8 kBq) resulted in a dramatic therapeutic response coupled with little signs of overt toxicity. In this context, H_2MacropaSq could be considered a superior chelator to DOTA for [^{225}Ac]Ac^{III} based immunotherapy. Further toxicology and dosimetry studies are required to guide potential translation to the clinic. It is likely that H_2MacropaSqOEt could be used to modify other antibodies, providing a readily adaptable platform for actinium-225 based immunotherapy.

Data availability

All experimental data is included in the ESI.†

Author contributions

The manuscript was written through contributions of all authors. All authors have given approval to the final version of the manuscript.

Conflicts of interest

K. A. M., C. W. W., A. M. S., and P. S. D. are listed as inventors of intellectual property that relate to aspects of this work. Telix Pharmaceuticals provided partial financial support. P. S. D. has received research funding from Telix Pharmaceuticals and Clarity Pharmaceuticals and has financial interests in Telix Pharmaceuticals and Clarity Pharmaceuticals.

Acknowledgements

We thank Dr Asif Noor (University of Melbourne) for his expertise and assistance in the ELISA assay. We acknowledge the Bio21 Mass Spectrometry and Proteomics Facility for instrumentation and technical support. Financial support from the Australian Cancer Research Foundation supported the purchase of an NMR spectrometer used in this work. Girentuximab was provided by Telix Pharmaceuticals. Dr Michael Wheatcroft and Dr Divesh Kumar both of Telix Pharmaceuticals are thanked for their support of this work. We acknowledge Austin Anatomical Pathology for sectioning and embedding the tumors, spleens, and kidneys; and the ACRF Centre for Imaging the Tumour Microenvironment for the use of the confocal microscope and slide scanner. We thank the U.S. Department of Energy Isotope Program (managed by the Office of Isotope R&D and Production) for supplying actinium-225. All animal studies were approved by the Austin Health Animal Ethics Committee. This research was funded in part by the Australian Research Council, the Australian Cancer Research Foundation, the National Health and Medical Research Council, the Victorian Cancer Council, and Telix Pharmaceuticals. K. A. M. acknowledges funding from an RTP (PhD) scholarship. AS is supported by NHMRC Investigator grant No. 1177837.

References

1 A. Sabet, K. Ezziddin, U.-F. Pape, K. Reichman, T. Haslerud, H. Ahmadzadehfar, H.-J. Biersack, J. Nagarajah and S. Ezziddin, Accurate assessment of long-term nephrotoxicity after peptide receptor radionuclide therapy with ^{177}Lu-octreotate, *Eur. J. Nucl. Med. Mol. Imag.*, 2014, **41**, 505–510.

2 J.-M. Beauregard, M. S. Hofman, G. Kong and R. J. Hicks, The tumour sink effect on the biodistribution of ^{68}Ga-DOTA-octreotate: implications for peptide receptor radionuclide therapy, *Eur. J. Nucl. Med. Mol. Imag.*, 2012, **39**, 50–56.

3 S. A. Deppen, J. Blume, A. J. Bobbey, C. Shah, M. M. Graham, P. Lee, D. Delbeke and R. C. Walker, ^{68}Ga-DOTATATE compared with ^{111}In-DTPA-octreotide and conventional imaging for pulmonary and gastroenteropancreatic neuroendocrine tumors: a systematic review and meta-analysis, *J. Nucl. Med.*, 2016, **57**, 872–878.

4 U. Hennrich and M. Benešová, [^{68}Ga]Ga-DOTA-TOC: The First FDA-Approved ^{68}Ga-Radiopharmaceutical for PET Imaging, *Pharmaceuticals*, 2020, **13**, 38.

5 R. Kashyap, M. S. Hofman, M. Michael, G. Kong, T. Akhurst, P. Eu, D. Zannino and R. J. Hicks, Favourable outcomes of ^{177}Lu-octreotate peptide receptor chemoradionuclide therapy in patients with FDG-avid neuroendocrine tumours, *Eur. J. Nucl. Med. Mol. Imag.*, 2015, **42**, 176–185.

6 G. Kong and R. J. Hicks, Peptide Receptor Radiotherapy: Current Approaches and Future Directions, *Curr. Treat. Options Oncol.*, 2019, **20**, 77.

7 O. Sartor, J. de Bono, K. N. Chi, K. Fizazi, K. Herrmann, K. Rahbar, S. T. Tagawa, L. T. Nordquist, N. Vaishampayan, G. El-Haddad, C. H. Park, T. M. Beer, A. Armour, W. J. Pérez-Contreras, M. DeSilvio, E. Kpamegan, G. Gericke, R. A. Messmann, M. J. Morris and B. J. Krause, Lutetium-177-PSMA-617 for Metastatic Castration-Resistant Prostate Cancer, *N. Engl. J. Med.*, 2021, **385**, 1091–1103.

8 C. Kratochwil, A. Afshar-Oromieh, K. Kopka, U. Haberkorn and F. L. Giesel, Current Status of Prostate-Specific Membrane Antigen Targeting in Nuclear Medicine: Clinical Translation of Chelator Containing Prostate-Specific Membrane Antigen Ligands Into Diagnostics and Therapy for Prostate Cancer, *Semin. Nucl. Med.*, 2016, **46**, 405–418.

9 W. P. Fendler, S. Reinhardt, H. Ilhan, A. Delker, G. Böning, F. J. Gildehaus, C. Stief, P. Bartenstein, C. Gratzke, S. Lehner and A. Rominger, Preliminary experience with dosimetry, response and patient reported outcome after ^{177}Lu-PSMA-617 therapy for metastatic castration-resistant prostate cancer, *Oncotarget*, 2017, **8**, 3581–3590.

10 J. Violet, P. Jackson, J. Ferdinandus, S. Sandhu, T. Akhurst, A. Iravani, G. Kong, A. R. Kumar, S. P. Thang, P. Eu, M. Scalzo, D. Murphy, S. Williams, R. J. Hicks and M. S. Hofman, Dosimetry of ^{177}Lu-PSMA-617 in Metastatic Castration-Resistant Prostate Cancer: Correlations Between Pretherapeutic Imaging and Whole-Body Tumor Dosimetry with Treatment Outcomes, *J. Nucl. Med.*, 2019, **60**, 517.

11 K. A. Morgan, S. E. Rudd, A. Noor and P. S. Donnelly, Theranostic Nuclear Medicine with Gallium-68, Lutetium-177, Copper-64/67, Actinium-225, and Lead-212/203 Radionuclides, *Chem. Rev.*, 2023, **123**, 12004–12035.

12 S. B. Dowd and E. R. Tilson, *Practical radiation protection and applied radiobiology*, W. B. Saunders, Philadelphia, 2nd edn, 1999, p. xvi, 352.

13 A. H. Staudacher, V. Liapis and M. P. Brown, Therapeutic targeting of tumor hypoxia and necrosis with antibody α-radioconjugates, *Antibody Ther.*, 2018, **1**, 55–63.

14 M. R. Raju, Y. Eisen, S. Carpenter and W. C. Inkret, Radiobiology of alpha particles. III. Cell inactivation by alpha-particle traversals of the cell nucleus, *Radiat. Res.*, 1991, **128**, 204–209.

15 A. I. Kassis, C. R. Harris, S. J. Adelstein, T. J. Ruth, R. Lambrecht and A. P. Wolf, The *in vitro* radiobiology of astatine-211 decay, *Radiat. Res.*, 1986, **105**, 27–36.

16 S. Poty, L. C. Francesconi, M. R. McDevitt, M. J. Morris and J. S. Lewis, α-Emitters for Radiotherapy: From Basic Radiochemistry to Clinical Studies-Part 1, *J. Nucl. Med.*, 2018, **59**, 878–884.

17 G. L. Semenza, Life with oxygen, *Science*, 2007, **318**, 62–64.

18 L. E. Huang, J. Gu, M. Schau and H. F. Bunn, Regulation of hypoxia-inducible factor 1alpha is mediated by an O_2-dependent degradation domain *via* the ubiquitin-proteasome pathway, *Proc. Natl. Acad. Sci. U. S. A.*, 1998, **95**, 7987–7992.

19 G. L. Wang, B. H. Jiang, E. A. Rue and G. L. Semenza, Hypoxia-inducible factor 1 is a basic-helix-loop-helix-PAS heterodimer regulated by cellular O2 tension, *Proc. Natl. Acad. Sci. U. S. A.*, 1995, **92**, 5510–5514.

20 M. Krieg, R. Haas, H. Brauch, T. Acker, I. Flamme and K. H. Plate, Up-regulation of hypoxia-inducible factors HIF-1alpha and HIF-2alpha under normoxic conditions in renal carcinoma cells by von Hippel-Lindau tumor suppressor gene loss of function, *Oncogene*, 2000, **19**, 5435–5443.

21 P. Vaupel, The role of hypoxia-induced factors in tumor progression, *Oncologist*, 2004, **9**(suppl 5), 10–17.

22 Y. H. Shi and W. G. Fang, Hypoxia-inducible factor-1 in tumour angiogenesis, *World J. Gastroenterol.*, 2004, **10**, 1082–1087.

23 S. C. Clifford, A. H. Prowse, N. A. Affara, C. H. Buys and E. R. Maher, Inactivation of the von Hippel-Lindau (VHL) tumour suppressor gene and allelic losses at chromosome arm 3p in primary renal cell carcinoma: evidence for a VHL-independent pathway in clear cell renal tumourigenesis, *Genes, Chromosomes Cancer*, 1998, **22**, 200–209.

24 E. Oosterwijk, D. J. Ruiter, P. J. Hoedemaeker, E. K. Pauwels, U. Jonas, J. Zwartendijk and S. O. Warnaar, Monoclonal antibody G 250 recognizes a determinant present in renal-cell carcinoma and absent from normal kidney, *Int. J. Cancer*, 1986, **38**, 489–494.

25 K. Grabmaier, J. L. M. Vissers, M. C. A. De Weijert, J. C. Oosterwijk-Wakka, A. Van Bokhoven, R. H. Brakenhoff, E. Noessner, P. A. Mulders, G. Merkx, C. G. Figdor, G. J. Adema and E. Oosterwijk, Molecular cloning and immunogenicity of renal cell carcinoma-associated antigen G250, *Int. J. Cancer*, 2000, **85**, 865–870.

26 B. C. Leibovich, Y. Sheinin, C. M. Lohse, R. H. Thompson, J. C. Cheville, J. Zavada and E. D. Kwon, Carbonic anhydrase IX is not an independent predictor of outcome for patients with clear cell renal cell carcinoma, *J. Clin. Oncol.*, 2007, **25**, 4757–4764.

27 J. C. Oosterwijk-Wakka, O. C. Boerman, P. F. Mulders and E. Oosterwijk, Application of monoclonal antibody G250 recognizing carbonic anhydrase IX in renal cell carcinoma, *Int. J. Mol. Sci.*, 2013, **14**, 11402–11423.

28 C. P. Potter and A. L. Harris, Diagnostic, prognostic and therapeutic implications of carbonic anhydrases in cancer, *Br. J. Cancer*, 2003, **89**, 2–7.

29 E. Oosterwijk, F. M. Debruyne and J. A. Schalken, The use of monoclonal antibody G250 in the therapy of renal-cell carcinoma, *Semin. Oncol.*, 1995, **22**, 34–41.

30 H. Uemura, Y. Nakagawa, K. Yoshida, S. Saga, K. Yoshikawa, Y. Hirao and E. Oosterwijk, MN/CA IX/G250 as a potential target for immunotherapy of renal cell carcinomas, *Br. J. Cancer*, 1999, **81**, 741–746.

31 C. H. Muselaers, M. J. Boers-Sonderen, T. J. van Oostenbrugge, O. C. Boerman, I. M. Desar, A. B. Stillebroer, S. F. Mulder, C. M. van Herpen, J. F. Langenhuijsen, E. Oosterwijk, W. J. Oyen and P. F. Mulders, Phase 2 Study of Lutetium 177-Labeled Anti-Carbonic Anhydrase IX Monoclonal Antibody Girentuximab in Patients with Advanced Renal Cell Carcinoma, *Eur. Urol.*, 2016, **69**, 767–770.

32 C. Wulbrand, C. Seidl, F. C. Gaertner, F. Bruchertseifer, A. Morgenstern, M. Essler and R. Senekowitsch-Schmidtke, Alpha-particle emitting ^{213}Bi-anti-EGFR immunoconjugates eradicate tumor cells independent of oxygenation, *PLoS One*, 2013, **8**, e64730.

33 P. E. Borchardt, R. R. Yuan, M. Miederer, M. R. McDevitt and D. A. Scheinberg, Targeted actinium-225 *in vivo* generators for therapy of ovarian cancer, *Cancer Res.*, 2003, **63**, 5084–5090.

34 F. E. Escorcia, E. Henke, M. R. McDevitt, C. H. Villa, P. Smith-Jones, R. G. Blasberg, R. Benezra and D. A. Scheinberg, Selective killing of tumor neovasculature paradoxically improves chemotherapy delivery to tumors, *Cancer Res.*, 2010, **70**, 9277–9286.

35 A. s. M. Ballangrud, W.-H. Yang, S. Palm, R. Enmon, P. E. Borchardt, V. A. Pellegrini, M. R. McDevitt, D. A. Scheinberg and G. Sgouros, Alpha-Particle Emitting Atomic Generator (Actinium-225)-Labeled Trastuzumab (Herceptin) Targeting of Breast Cancer Spheroids: Efficacy *versus* HER2/neu Expression, *Clin. Cancer Res.*, 2004, **10**, 4489–4497.

36 W. F. Maguire, M. R. McDevitt, P. M. Smith-Jones and D. A. Scheinberg, Efficient 1-step radiolabeling of monoclonal antibodies to high specific activity with ^{225}Ac for alpha-particle radioimmunotherapy of cancer, *J. Nucl. Med.*, 2014, **55**, 1492–1498.

37 R. I. J. Merkx, M. Rijpkema, G. M. Franssen, A. Kip, B. Smeets, A. Morgenstern, F. Bruchertseifer, E. Yan, M. P. Wheatcroft, E. Oosterwijk, P. F. A. Mulders and S. Heskamp, Carbonic Anhydrase IX-Targeted α-Radionuclide Therapy with ^{225}Ac Inhibits Tumor Growth in a Renal Cell Carcinoma Model, *Pharmaceuticals*, 2022, **15**, 570.

38 R. M. Smith and A. E. Martell, *Critical Stability Constants: Second Supplement*, in Springer, Plenum, New York, London, 1989, vol. 6, p. 643.

39 N. A. Thiele, V. Brown, J. M. Kelly, A. Amor-Coarasa, U. Jermilova, S. N. MacMillan, A. Nikolopoulou, S. Ponnala, C. F. Ramogida, A. K. H. Robertson, C. Rodriguez-Rodriguez, P. Schaffer, C. Williams Jr, J. W. Babich, V. Radchenko and J. J. Wilson, An Eighteen-Membered Macrocyclic Ligand for Actinium-225 Targeted Alpha Therapy, *Angew. Chem., Int. Ed.*, 2017, **56**, 14712–14717.

40 A. Roca-Sabio, M. Mato-Iglesias, D. Esteban-Gomez, E. Toth, A. de Blas, C. Platas-Iglesias and T. Rodriguez-Blas, Macrocyclic receptor exhibiting unprecedented selectivity for light lanthanides, *J. Am. Chem. Soc.*, 2009, **131**, 3331–3341.

41 A. Hu and J. J. Wilson, Advancing Chelation Strategies for Large Metal Ions for Nuclear Medicine Applications, *Acc. Chem. Res.*, 2022, **55**, 904–915.

42 K. J. Kadassery, A. P. King, S. Fayn, K. E. Baidoo, S. N. MacMillan, F. E. Escorcia and J. J. Wilson, H2BZmacropa-NCS: A Bifunctional Chelator for Actinium-225 Targeted Alpha Therapy, *Bioconjugate Chem.*, 2022, **33**, 1222–1231.

43 M. Mato-Iglesias, A. Roca-Sabio, Z. Pálinkás, D. Esteban-Gómez, C. Platas-Iglesias, É. Tóth, A. de Blas and T. Rodríguez-Blas, Lanthanide Complexes Based on a 1,7-Diaza-12-crown-4 Platform Containing Picolinate Pendants: A New Structural Entry for the Design of Magnetic Resonance Imaging Contrast Agents, *Inorg. Chem.*, 2008, **47**, 7840–7851.

44 S. E. Rudd, P. Roselt, C. Cullinane, R. J. Hicks and P. S. Donnelly, A desferrioxamine B squaramide ester for the incorporation of zirconium-89 into antibodies, *Chem. Commun.*, 2016, **52**, 11889–11892.

45 R. I. Storer, C. Aciro and L. H. Jones, Squaramides: physical properties, synthesis and applications, *Chem. Soc. Rev.*, 2011, **40**, 2330–2346.

46 F. Reissig, D. Bauer, K. Zarschler, Z. Novy, K. Bendova, M. C. Ludik, K. Kopka, H. J. Pietzsch, M. Petrik and C. Mamat, Towards Targeted Alpha Therapy with Actinium-225: Chelators for Mild Condition Radiolabeling and Targeting PSMA-A Proof of Concept Study, *Cancers*, 2021, **13**, 1974.

47 V. V. Rostovtsev, L. G. Green, V. V. Fokin and K. B. Sharpless, A stepwise huisgen cycloaddition process: copper(I)-catalyzed regioselective "ligation" of azides and terminal alkynes, *Angew. Chem., Int. Ed.*, 2002, **41**, 2596–2599.

48 C. W. Tornøe, C. Christensen and M. Meldal, Peptidotriazoles on solid phase: [1,2,3]-triazoles by regiospecific copper(i)-catalyzed 1,3-dipolar cycloadditions of terminal alkynes to azides, *J. Org. Chem.*, 2002, **67**, 3057–3064.

49 W. J. Cannan and D. S. Pederson, Mechanisms and Consequences of Double-Strand DNA Break Formation in Chromatin, *J. Cell. Physiol.*, 2016, **231**, 3–14.

50 M. Christmann, M. T. Tomicic, W. P. Roos and B. Kaina, Mechanisms of human DNA repair: an update, *Toxicology*, 2003, **193**, 3–34.

51 S. J. Collis, T. L. DeWeese, P. A. Jeggo and A. R. Parker, The life and death of DNA-PK, *Oncogene*, 2005, **24**, 949–961.

52 J. E. Haber, Partners and pathwaysrepairing a double-strand break, *Trends Genet.*, 2000, **16**, 259–264.

53 T. Rich, R. L. Allen and A. H. Wyllie, Defying death after DNA damage, *Nature*, 2000, **407**, 777–783.

54 G. C. Smith and S. P. Jackson, The DNA-dependent protein kinase, *Genes Dev.*, 1999, **13**, 916–934.

55 W. M. Bonner, C. E. Redon, J. S. Dickey, A. J. Nakamura, O. A. Sedelnikova, S. Solier and Y. Pommier, GammaH2AX and cancer, *Nat. Rev. Cancer*, 2008, **8**, 957–967.

56 C. Redon, D. Pilch, E. Rogakou, O. Sedelnikova, K. Newrock and W. Bonner, Histone H2A variants H2AX and H2AZ, *Curr. Opin. Genet. Dev.*, 2002, **12**, 162–169.

57 E. P. Rogakou, C. Boon, C. Redon and W. M. Bonner, Megabase chromatin domains involved in DNA double-strand breaks in vivo, *J. Cell Biol.*, 1999, **146**, 905–916.

58 D. V. Firsanov, L. V. Solovjeva and M. P. Svetlova, H2AX phosphorylation at the sites of DNA double-strand breaks in cultivated mammalian cells and tissues, *Clin. Epigenet.*, 2011, **2**, 283–297.

59 A. J. Nakamura, V. A. Rao, Y. Pommier and W. M. Bonner, The complexity of phosphorylated H2AX foci formation and DNA repair assembly at DNA double-strand breaks, *Cell Cycle*, 2010, **9**, 389–397.

60 F. Graf, J. Fahrer, S. Maus, A. Morgenstern, F. Bruchertseifer, S. Venkatachalam, C. Fottner, M. M. Weber, J. Huelsenbeck, M. Schreckenberger, B. Kaina and M. Miederer, DNA double strand breaks as predictor of efficacy of the alpha-particle emitter Ac-225 and the electron emitter Lu-177 for somatostatin receptor targeted radiotherapy, *PLoS One*, 2014, **9**, e88239.

61 A. Ivashkevich, C. E. Redon, A. J. Nakamura, R. F. Martin and O. A. Martin, Use of the gamma-H2AX assay to monitor DNA damage and repair in translational cancer research, *Cancer Lett.*, 2012, **327**, 123–133.

62 B. Meyer, K. O. Voss, F. Tobias, B. Jakob, M. Durante and G. Taucher-Scholz, Clustered DNA damage induces pan-nuclear H2AX phosphorylation mediated by ATM and DNA-PK, *Nucleic Acids Res.*, 2013, **41**, 6109–6118.

63 P. Workman, E. O. Aboagye, F. Balkwill, A. Balmain, G. Bruder, D. J. Chaplin, J. A. Double, J. Everitt, D. A. H. Farningham, M. J. Glennie, L. R. Kelland, V. Robinson, I. J. Stratford, G. M. Tozer, S. Watson, S. R. Wedge and S. A. Eccles, An *ad hoc* committee of the National Cancer Research, I. Guidelines for the welfare and use of animals in cancer research, *Br. J. Cancer*, 2010, **102**, 1555–1577.